AIAA JOURNAL
Vol. 34, No. 2, February 1996

Postprocess Method Using Displacement Field of Higher Order Laminated Composite Plate Theory

Maenghyo Cho* and Ji-Heon Kim†
Inha University, Inchon 402-751, Republic of Korea

Simplified higher order plate theories satisfy the transverse shear stress continuity conditions as well as the kinematic continuity conditions. Thus, they provide realistic displacement fields with the small number of dependent variables. These theories require tedious computations, however, since their in-plane displacement field is more complicated than the first-order shear theory. In this study, a simple and economical method is proposed without loss of accuracy of solutions. This method consists of two steps. First is to obtain the relationship between rotational angles of first order shear deformation plate theory (FOPT) and efficient higher order plate theory (EHOPT). Second is to obtain accurate displacement and stress fields from the first-order shear deformation plate theory solution by using EHOPT displacement fields as a postprocessor. Cylindrical bending problems demonstrate economical and accurate solution of laminated composite plates provided by the present method.

I. Introduction

INCREASINGLY in modern aircraft construction, composite materials are being used in primary loading structures. In the analysis of laminated composites, a first-order shear deformation theory is adequate to estimate the global behavior. But for the strength analysis, accurate prediction of stresses is required as well. Many analysis techniques have been developed for predicting the behavior of a multilayered composite plate. Methods that can accurately predict not only the global behavior but also the through-the-thickness stress behavior, however, are rare.

In the past many plate theories have been developed. Historically, smeared displacement-based higher order theories were developed first.[2,3] The assumed in-plane displacement of these higher order theories is expressed in polynomial form. The degree of the assumed polynomial decides the order of the plate theory. The polynomial-based in-plane displacement field is at variance with the three-dimensional elasticity displacement field because it does not satisfy interface stress continuity and top and bottom surface static boundary conditions.

To obtain improved results, layerwise theories have been developed.[4–6] These are known to be fairly accurate since at each interface between layers, they allow a kink in the slope of deflection. Nevertheless, these theories have the drawback of requiring many degrees of freedom, depending on the number of layers.

Recently some attention has been paid to the simplified higher order theories.[1,7–11] By imposing transverse shear free conditions at top and bottom surfaces or imposing interface continuity conditions between layers, the number of dependent variables decreases. Extensive reviews can be found in Ref. 12 for higher order theories for laminated composite plates.

The in-plane displacement of an efficient higher order plate theory (EHOPT) developed by Cho and Parmeter[1] satisfies the top and bottom surface shear stress free conditions and interface stress continuity conditions. It needs only the same number of dependent variables as with the first-order shear deformation theory. It shows the capability of predicting accurate deformations and stresses with a small number of unknowns. The computation to obtain solutions, however, is still tedious and it requires C^1 continuity.

Received Feb. 28, 1995; presented as Paper 95-1209 at the AIAA/ASME/ASCE/AHS/ASC 36th Structures, Structural Dynamics, and Materials Conference, New Orleans, LA, April 10–13, 1995; revision received Aug. 19, 1995; accepted for publication Aug. 22, 1995.

*Full Time Lecturer, Department of Aerospace Engineering, 253 Yong-Hyun Dong, Nam-ku.
†Graduate Research Assistant, Department of Aerospace Engineering, 253 Yong-Hyun Dong, Nam-ku.

The objective of the present study is to develop a postprocess method that is based on only the degrees of freedom of the first-order theory and, hence, is best suited for the general purpose environment.

II. Matching the Rotational Variables

The displacement field of the first-order shear deformation theory is given as follows:

$$u_\alpha = u_\alpha^0 + \psi_\alpha z \qquad u_3 = w(x_1, x_2) \tag{1}$$

where u_α^0 and w are the in-plane stretching and out-of-plane deflection, respectively, in the midplane. The rotation variable ψ_α is the angle at the midsurface.

The transverse shear strain can be expressed from the strain-displacement relationship,

$$\begin{aligned}\gamma_{3\alpha} &= \frac{\partial u_\alpha}{\partial z} + \frac{\partial u_3}{\partial x_\alpha} \\ &= \psi_\alpha + w_{,\alpha} = \varphi_\alpha\end{aligned} \tag{2}$$

The in-plane displacement field given in Eq. (1) is a straight line through the whole thickness. Thus, it does not satisfy transverse shear free conditions at the top and bottom surface, nor the interface continuity conditions.

In EHOPT, zig-zag linear function is superimposed to the globally cubic varying displacement to satisfy static continuity, as well as geometric continuity conditions. We start with the following displacement field for a symmetric laminated plate:

$$\begin{aligned}u_\alpha &= u_\alpha^0 + \psi_\alpha z + \xi_\alpha z^2 + \phi_\alpha z^3 + \sum_{k=1}^{N/2-1} S_\alpha^k \\ &\quad \times [(z - z_k)H(z - z_k) - (-z - z_k)H(-z - z_k)] \\ u_3 &= w(x_1, x_2)\end{aligned} \tag{3}$$

where N is the number of layers and $H(z - z_k)$ is the Heaviside unit step function. The configuration of the in-plane displacement field is given in Fig. 1.

The number of unknowns are reduced by imposing top and bottom surface transverse shear free conditions $\sigma_{3\alpha}|_{z=\pm(h/2)} = 0$,

$$\begin{aligned}\xi_\alpha &= 0 \\ \phi_\alpha &= -\frac{4}{3h^2}\left(w_{,\alpha} + \psi_\alpha + \sum_{k=1}^{N/2-1} S_\alpha^k\right)\end{aligned} \tag{4}$$

By applying interface transverse shear stress continuity conditions, in-plane interface slope kink angle S_α^k can be determined,

$$S_\alpha^k = a_{\alpha\gamma}^k(\psi_\gamma + w_{,\gamma}) \tag{5}$$

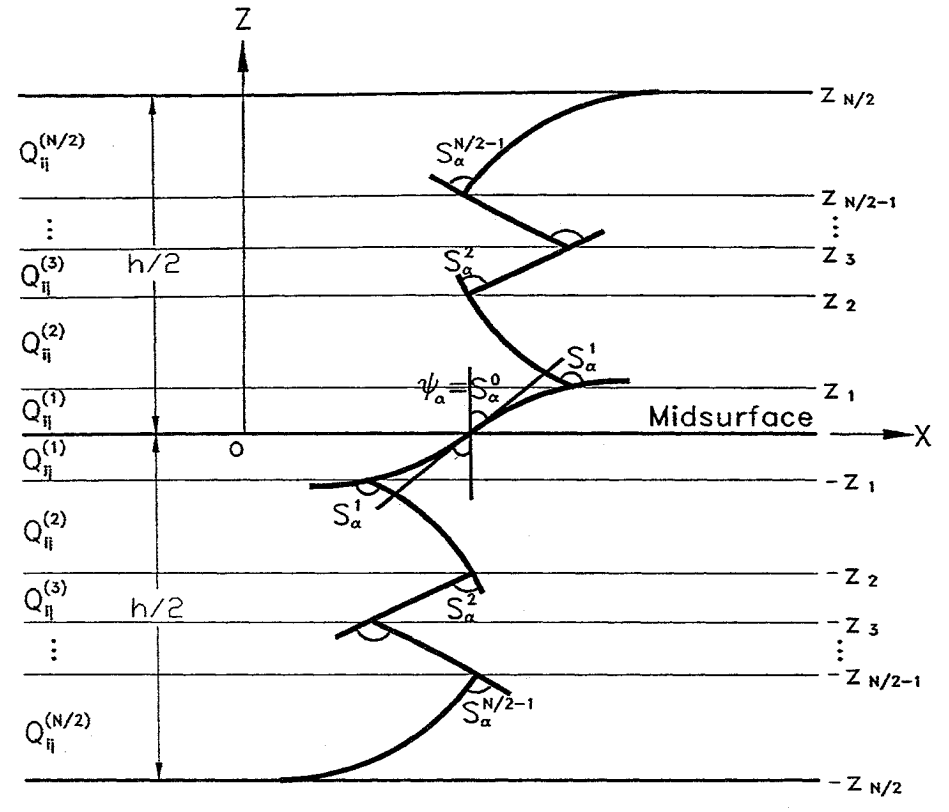

Fig. 1 Configuration of the in-plane displacement field.

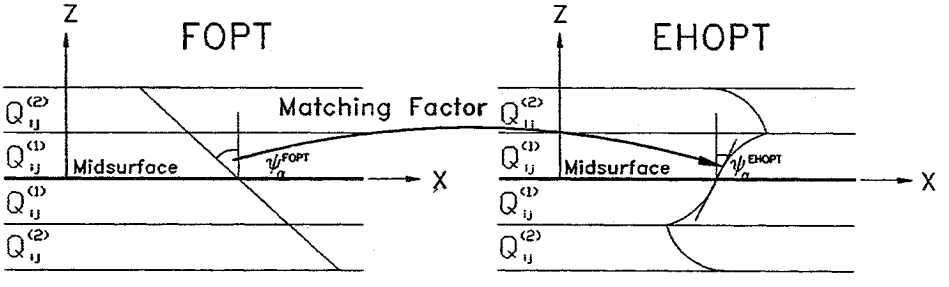

Fig. 2 Matching rotational variables.

where $a^k_{\alpha\gamma}$ can be determined by the layer transverse material properties and layer thickness. The detailed derivation of Eq. (5) can be found in Ref. 1.

The displacement field in Eq. (3) now reduces to

$$u_\alpha = u^0_\alpha + \psi_\alpha z - \frac{4z^3}{3h^2}\left[w_{,\alpha} + \psi_\alpha + \sum_{k=1}^{N/2-1} a^k_{\alpha\gamma}(\psi_\gamma + w_{,\gamma})\right] + \sum_{k=1}^{N/2-1} a^k_{\alpha\gamma}(\psi_\gamma + w_{,\gamma})[(z - z_k)H(z - z_k) - (-z - z_k)H(-z - z_k)]$$

$$u_3 = w(x_1, x_2) \tag{6}$$

Transverse shear strain is obtained by the strain-displacement relationship,

$$\gamma_{3\alpha} = \frac{\partial u_\alpha}{\partial z} + \frac{\partial u_3}{\partial x_\alpha} = \varphi_\alpha - \frac{4z^2}{h^2}\left[\varphi_\alpha + \sum_{k=1}^{N/2-1} a^k_{\alpha\gamma}\varphi_\gamma\right] + \sum_{k=1}^{N/2-1} a^k_{\alpha\gamma}\varphi_\gamma[H(z - z_k) + H(-z - z_k)] \tag{7}$$

where $\varphi_\alpha = w_{,\alpha} + \psi_\alpha$.

Both the transverse shear strain of the first-order shear theory and that of EHOPT are expressed in terms of the variable φ_α. Thus, from these two plate theories, the variable φ_α of the EHOPT can be obtained in terms of the variable φ_α of first order plate theory (FOPT) by assuming the transverse shear energy of EHOPT and FOPT is equal. In Fig. 2, the matching rotational variables are depicted.

The transverse shear strain energy of the laminated composites are given as

$$U_S = \frac{1}{2}\sum_{k=1}^{N/2}\int_{z_{k-1}}^{z_k} 2\begin{Bmatrix}\gamma^k_{32}\\ \gamma^k_{31}\end{Bmatrix}^T\begin{bmatrix}Q^k_{44} & Q^k_{45}\\ Q^k_{45} & Q^k_{55}\end{bmatrix}\begin{Bmatrix}\gamma^k_{32}\\ \gamma^k_{31}\end{Bmatrix} dz \tag{8}$$

To obtain more accurate global deformations, a shear correction factor[13] is used in the FOPT. For the cross-ply laminated composites,

$$U_S = \frac{1}{2}\int_{-h/2}^{h/2}\left(Q^k_{44}\gamma^2_{32} + Q^k_{55}\gamma^2_{31}\right) dz \tag{9}$$

Let us assume that the shear energy of FOPT is equal to that of EHOPT,

$$U_S^{\text{FOPT}} = U_S^{\text{EHOPT}} \tag{10}$$

The variable $\varphi_\alpha^{\text{EHOPT}}$ can be expressed in terms of $\varphi_\alpha^{\text{FOPT}}$ with the linear factor C_α,

$$\varphi_\alpha^{(\text{EHOPT})} = C_\alpha\varphi_\alpha^{(\text{FOPT})} \tag{11}$$

with no summation in α. Then substituting Eq. (11) to Eq. (6), improved in-plane displacements are stresses are obtained by using

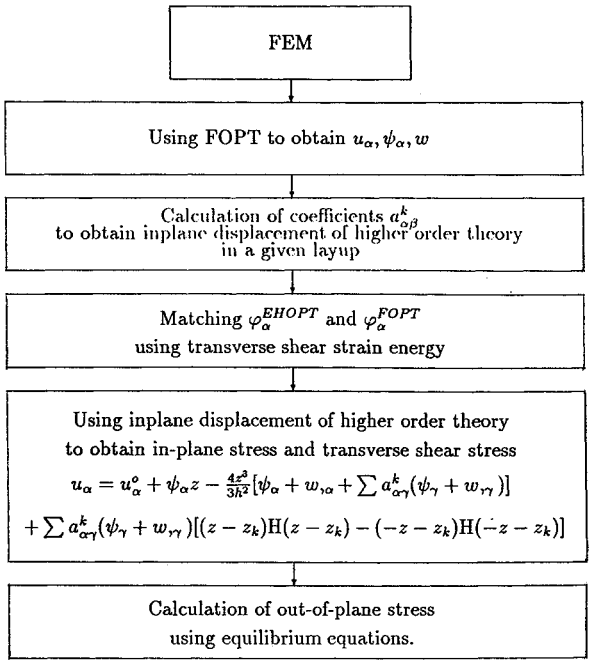

Fig. 3 Flow chart.

only the FOPT solution. The detailed calculation flow chart is given in Fig. 3.

III. Numerical Examples of Cylindrical Bending Problem

To examine the accuracy of the proposed method, cylindrical bending of plates is considered. The cylindrical bending elasticity solution was proposed by Pagano.[14] In many higher order theories, the exact solutions are solved for this problem. Thus, it is easy to assess the present method by comparing it to other theories and exact elasticity solutions.

The boundary conditions for simply supported ends at $x = 0, L$ are

$$w = M_{11} = 0 \tag{12}$$

We assume that the applied transverse load p is sinusoidal

$$p(x) = p_0 \sin(\pi/L)x \tag{13}$$

The displacement solution of the first-order shear theory is given as

$$\begin{aligned} u^0 &= A\cos(m\pi/L)x \\ \psi_1 &= B\cos(m\pi/L)x \\ w &= C\sin(m\pi/L)x \end{aligned} \tag{14}$$

where

$$\begin{aligned} A &= \frac{B_{11}a^3 p_0}{m^3\pi^3\left(A_{11}D_{11} - B_{11}^2\right)} \\ B &= -\frac{A_{11}a^3 p_0}{m^3\pi^3\left(A_{11}D_{11} - B_{11}^2\right)} \\ C &= \frac{p_0 a^2}{m^2\pi^2}\left[\frac{A_{11}a^2}{m^2\pi^2\left(A_{11}D_{11} - B_{11}^2\right)} + \frac{1}{kA_{55}}\right] \end{aligned} \tag{15}$$

where k is a shear correction factor,

$$(A_{11}, B_{11}, D_{11}) = \int_{-h/2}^{h/2} \bar{Q}^k_{11}(1, z, z^2)\,dz \tag{16}$$

The material properties for the 0-deg layer are

$$E_1 = (25 \times 10^6 \text{ psi}) \qquad E_2 = (10^6 \text{ psi})$$

$$G_{12} = G_{13} = (0.5 \times 10^6 \text{ psi}) \qquad G_{23} = (0.2 \times 10^6 \text{ psi})$$

$$\nu_{12} = \nu_{13} = \nu_{23} = 0.25$$

To facilitate comparison with other known theories, the following nondimensional parameters are defined for Tables 1 and 2:

$$\sigma^*_x = \frac{\sigma_x}{Q_0 \sin(\pi/L)x}, \qquad \sigma^*_{xz} = \frac{\sigma_{31}}{Q_0 \cos(\pi/L)x} \tag{17}$$

where

$$Q_0 = \frac{p_0}{2}$$

Other nondimensional parameters are defined following Pagano[14] for Figs. 4–6,

$$\begin{aligned} u^* &= \frac{E_T u(0, z)}{h(p_0)} \qquad & \sigma_1 &= \frac{\sigma_1(l/2, z)}{p_0} \\ \tau_{31} &= \frac{\tau_{31}(0, z)}{p_0} \qquad & \sigma_{zz} &= \frac{\sigma_{zz}(l/2, z)}{p_0} \end{aligned} \tag{18}$$

It is assumed that the out-of-plane deflection w of EHOPT is same as that of FOPT. In the following, rotational variables are corrected to get the improved in-plane displacement and stress,

$$\psi^{(\text{EHOPT})}_\alpha = \varphi_\alpha - w^{(\text{FOPT})}_{,\alpha} \tag{19}$$

Nondimensional deflections are calculated quite accurately in both theories.

Tables 1 and 2 show the comparison of the present results and of other theories for $(0/90)_s$ lamination layup. In-plane stresses are significantly improved by the present method compared to the FOPT given in Table 1. In-plane stresses are slightly less accurate than those of EHOPT and are more accurate than those of the smeared higher order theory.

The transverse shear stress distribution can be obtained in two ways: by the constitutive equations and by integrating the equilibrium equation. In the present study, the constitutive equation approach gives less accurate transverse shear stress distribution than the equilibrium equation approach, as shown in Table 2. The qualitative behavior, however, is correct, and the transverse shear stress continuity condition and stress free conditions are satisfied as shown in Table 2.

Figures 4–6 for (0/90/0) lamination and thickness ratio $(L/h) = 4$. Even in the very thick plate case, the present method gives good

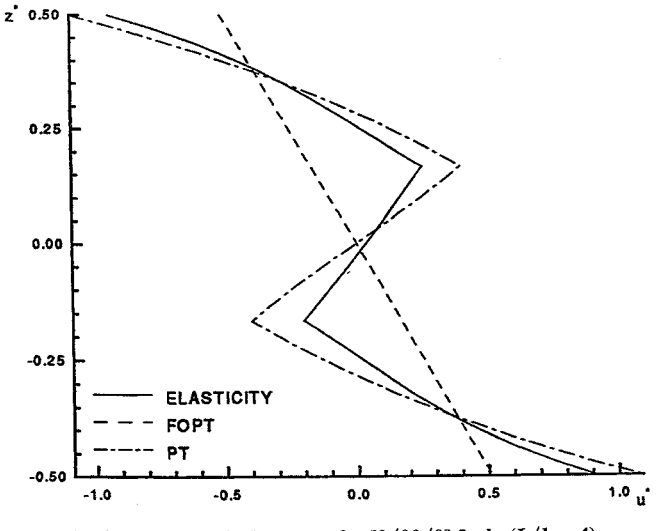

Fig. 4 In-plane displacement for [0/90/0] 3-ply (L/h = 4).

Table 1 Comparison of σ_x^* (axial stresses)

L/h	$z/2h$	Pagano[14]	PT	EHOPT[1]	Krishna (1987)	CLPT
25	0.2	6.6381	6.5452	6.5220	6.6212	7.3477
	0.4	13.2810	13.1405	13.0949	13.3376	14.6954
	0.5	16.6057	16.4726	16.4164	16.7613	18.3693
	0.5	411.2784	411.8150	410.4103	422.2264	431.6905
	0.6	503.6770	504.7125	503.1978	509.7459	517.9314
	0.8	691.6122	693.4838	691.7974	690.0948	690.5752
	1.0	884.9604	887.2678	885.4910	879.3870	863.2190
12.5	0.2	1.4629	1.3640	1.3440	1.5151	1.8369
	0.4	2.9302	2.7781	2.7384	3.1252	3.6739
	0.5	3.6668	3.5196	3.4704	3.9956	4.5923
	0.5	87.8467	87.9902	86.7602	98.4508	107.9024
	0.6	115.4014	116.1227	114.7301	121.2114	129.4828
	0.8	173.4500	175.3641	173.6697	172.0361	172.6474
	1.0	236.9496	239.6182	237.6618	231.7929	215.8047

Table 2 Comparison of σ_{xz}^* (transverse shear stresses)

L/h	$z/2h$	Pagano[14]	PT	EHOPT[1]	Krishna (1987)	PT[a]	EHOPT[a]	Krishna[a] (1987)
25	0.0	20.5395	21.1915	21.4815	17.7324	20.5868	20.5347	20.5699
	0.2	20.4978	20.7926	21.0771	17.0231	20.5457	20.4967	20.5283
	0.4	20.3726	19.5959	19.8641	14.8952	20.4221	20.3705	20.4030
	0.5	20.2787	18.6984	18.9543	13.2993	20.3291	20.2778	20.3086
	0.5	20.2787	18.6984	18.9543	33.2482	20.3291	20.2778	20.3086
	0.6	17.4048	15.9559	16.1743	28.3718	17.4501	17.4081	17.3814
	0.8	9.8995	8.9752	9.0981	15.9591	9.9263	9.9044	9.8508
12.5	0.0	10.1554	10.5957	10.6529	8.8448	10.2469	10.1440	10.2225
	0.2	10.1370	10.3963	10.4524	8.4910	10.2298	10.1271	10.2036
	0.4	10.0818	9.79795	9.8508	7.4296	10.1779	10.0760	10.1456
	0.5	10.0404	9.34919	9.3996	6.6336	10.1383	10.0370	10.1009
	0.5	10.0404	9.34919	9.3996	16.5840	10.1383	10.0370	10.1009
	0.6	8.7642	7.9780	8.0210	14.1517	8.8568	8.7719	8.7223
	0.8	5.1438	4.4876	4.5118	7.9603	5.2030	5.1570	5.0536

[a]Solution by integrating the equilibrium equation.

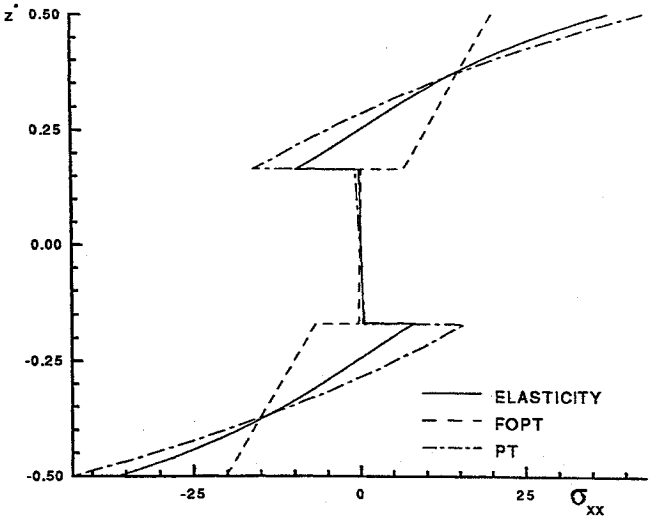

Fig. 5 In-plane normal stress for [0/90/0] 3-ply (L/h = 4).

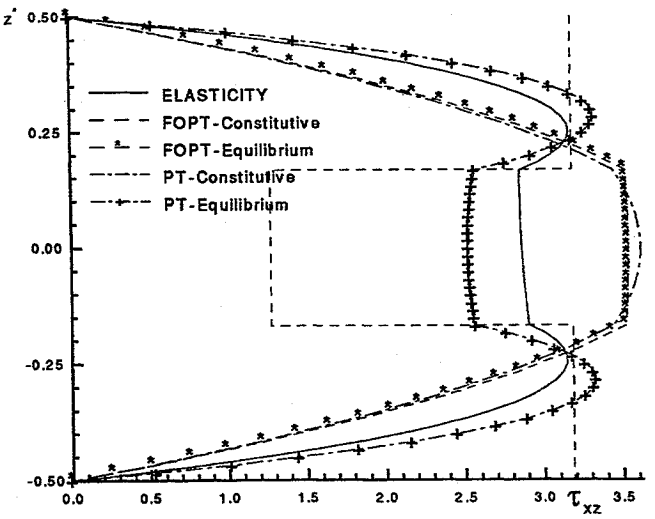

Fig. 6 Transverse shear stress for [0/90/0] 3-ply (L/h = 4).

results for displacements and stresses. In the axial stress distributions, the present method provides an improved stress prediction, especially at the interfaces and the top and bottom surfaces in which the first-order theory predictions of the axial stresses are not as accurate as the present method. Thus, the present method is advantageous in strength analysis because the maximum value of the axial stress usually occurs at such points.

To demonstrate the validity of the present method, the transverse shear strain energy and bending strain energy are calculated. In addition, relative percent errors between FOPT and Pagano's exact solution are calculated, along with relative percent error between EHOPT postprocessor and the exact solution, which are plotted in Fig. 7.

The transverse shear energy of the postprocessor in EHOPT must be equal to that of FOPT because we assumed they are same. The relative error of the shear energy between the exact solution and this theory is given in Fig. 7. As is shown in Fig. 7, if the aspect ratio (L/h) is 10, then the energy error of transverse shear is within 5%.

The discrepancy of the energy between postprocessor and the exact solution causes some deformation. The effect of deformation

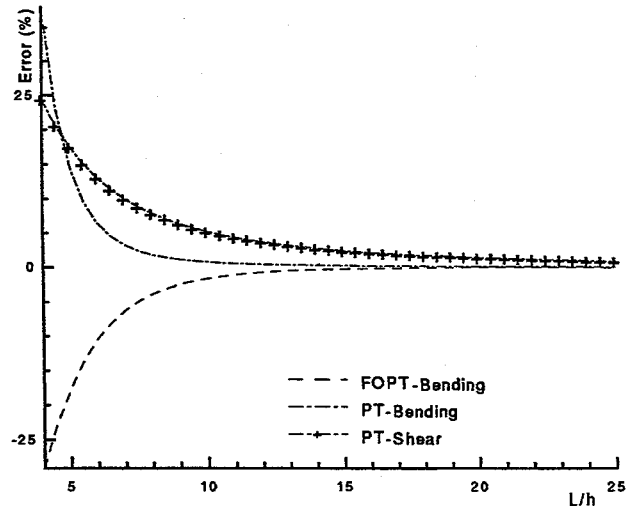

Fig. 7 Relative error of bending and shear strain energy for [0/90/0] 3-ply.

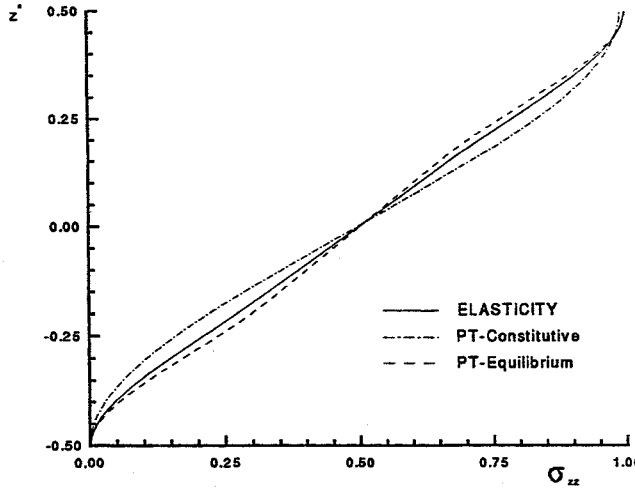

Fig. 8 Transverse normal stress obtained by integrating equilibrium equation for [0/90/0] 3-ply (L/h = 4); PT-constitutive, $\tau_{3\alpha}$ is calculated by constitutive equation approach and PT-equilibrium, $\tau_{3\alpha}$ is calculated by equilibrium equation approach.

due to the bending energy discrepancy, however, is not as significant as that due to the shear energy discrepancy. As is shown in Fig. 7, in the postprocessor of EHOPT, the bending energy error is within 5%, whereas the shear energy error is about 10% in the case of $(L/h) = 7$. This suggests that the importance of matching transverse shear-strain energy should be emphasized, whereas the effect of bending energy error can be regarded as less important.

The transverse normal stress may also significant in designing laminated composite structures. In Fig. 8, the calculation results of the transverse normal stresses are shown. In the transverse normal stress calculation, the method of integrating equilibrium equations is used. From the out-of-plane three-dimensional stress equilibrium equations,

$$\sigma_{zz} = -\int (\tau_{xz,x} + \tau_{yz,y})\, dz \tag{20}$$

The transverse shear stress can be obtained using constitutive equations and in-plane equilibrium equations. Constitutive-approached transverse shear stresses make the calculation of interlaminar normal stress σ_{zz} easier. The equilibrium-approached transverse shear stresses, however, provide more accurate interlaminar normal stress σ_{zz} even though the calculation involves higher order derivatives of deflection w.

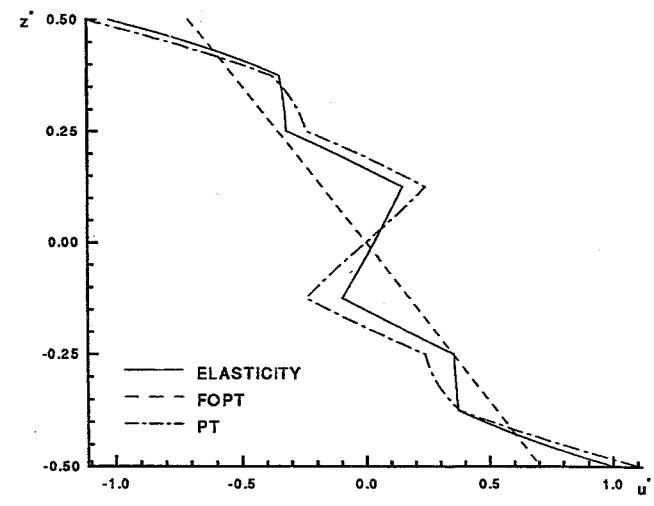

Fig. 9 In-plane displacement for $[0/90]_{2s}$ 8-ply (L/h = 4).

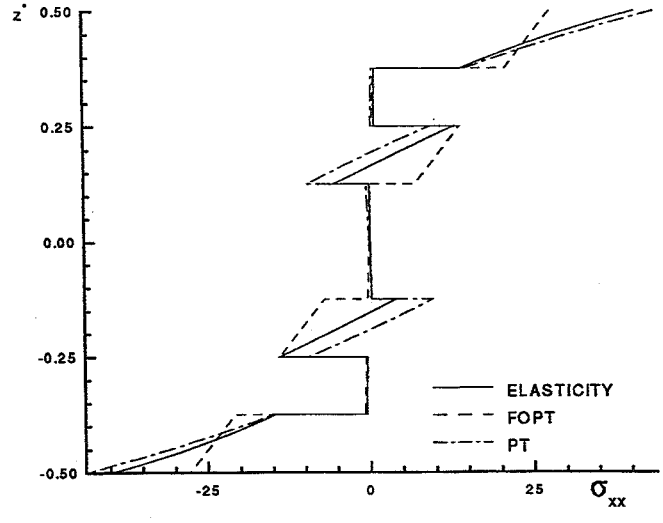

Fig. 10 In-plane normal stress $[0/90]_{2s}$ 8-ply (L/h = 4).

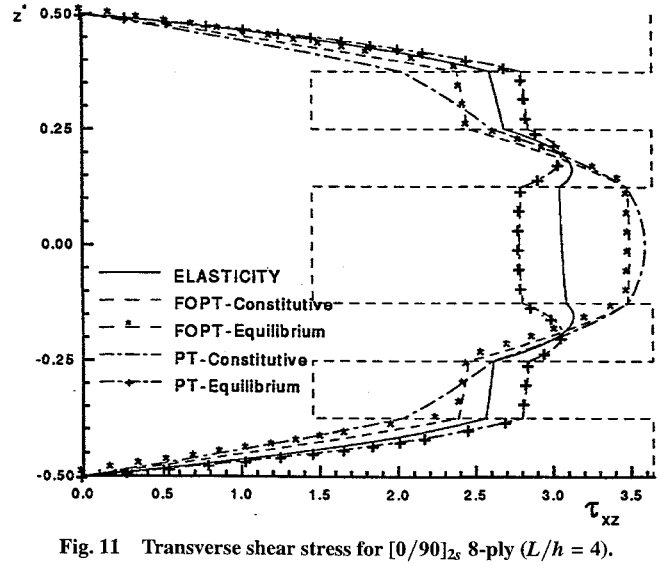

Fig. 11 Transverse shear stress for $[0/90]_{2s}$ 8-ply (L/h = 4).

To further assess the range of applicability of the present method, we consider the problem involving $(0/90)_{4s}$ 8-ply and $(0/90)_{8s}$ 16-ply.

In Figs. 9–11, the stresses and deformation of the 8-layer cross-ply problem are shown. The present postprocess method works successfully for the multilayered problem. It recovers quite accurately the in-plane stress and transverse shear stresses. Figure 12

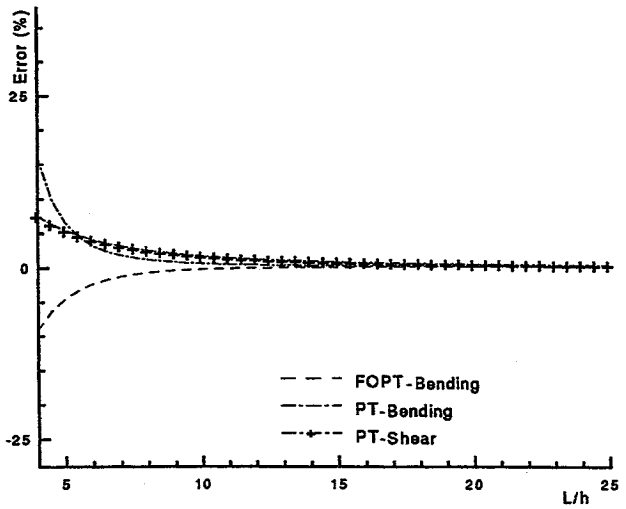

Fig. 12 Relative error of bending and shear strain energy for $[0/90]_{2s}$ 8-ply.

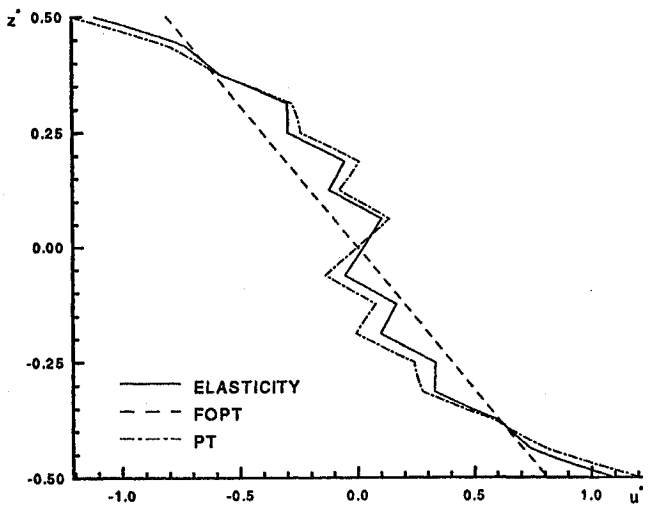

Fig. 13 In-plane displacement for $[0/90]_{4s}$ 16-ply (L/h = 4).

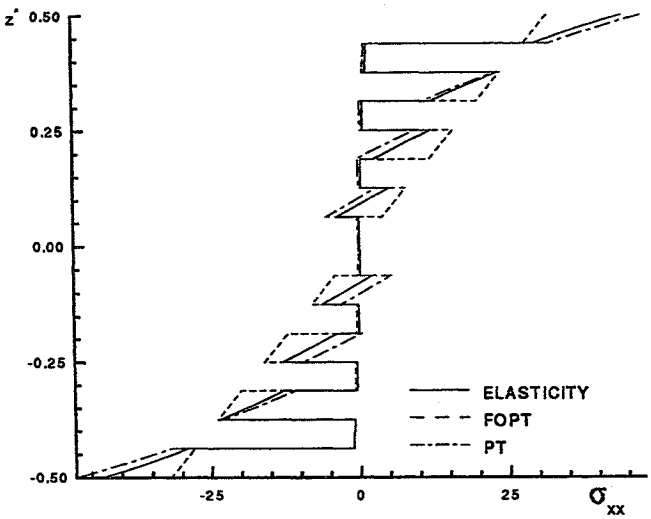

Fig. 14 In-plane normal stress for $[0/90]_{4s}$ 16-ply (L/h = 4).

shows relative bending and shear energy errors in the 8-layer cross-ply problem. As the number of plies increases, the error between the postprocessor method and the exact elasticity solution decreases.

In Figs. 13–15, the stresses and displacement through the thickness of the 16-layer cross-ply problem are shown. Even in thick range of application, (L/h) = 4, the present method predicts

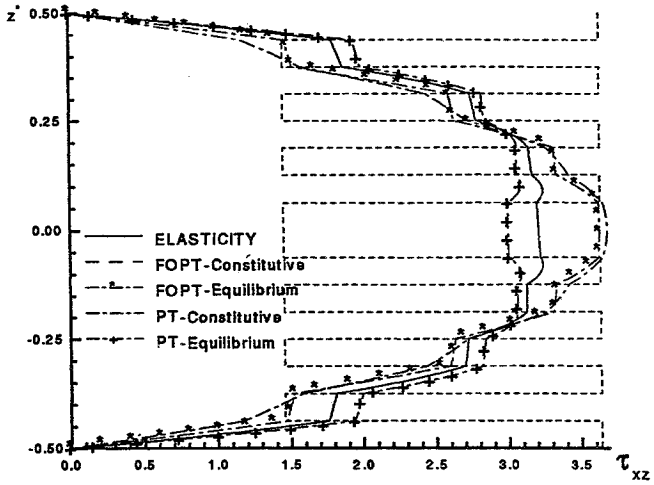

Fig. 15 Transverse shear stress for $[0/90]_{4s}$ 16-ply (L/h = 4).

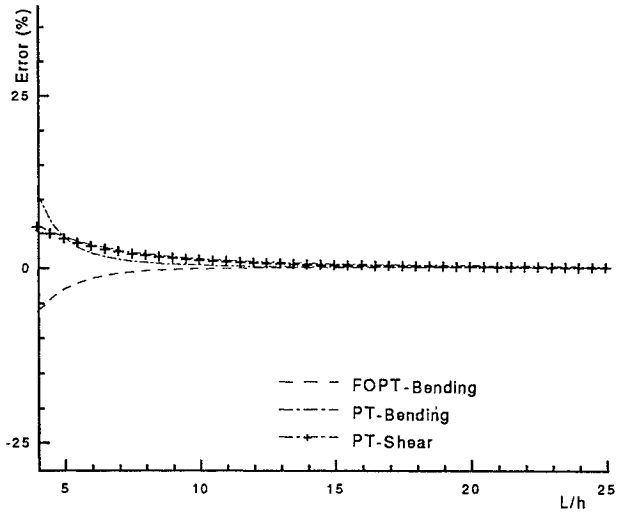

Fig. 16 Relative error of bending and shear strain energy for $[0/90]_{4s}$ 16-ply.

maximum in-plane stresses within 5% error, whereas FOPT predicts maximum in-plane stresses with more than 30% error. Transverse shear stresses are also accurately predicted by the present method using the equilibrium equation approach. Figure 16 shows the validity of the present method for the 16-layer cross-ply problem. If the aspect ratio (L/h) is larger than 5, both errors of the bending energy and of the shear energy is within 5%.

IV. Conclusions

In the present paper, a simple and economical methodology based on a first-order solution to exploit higher order effects by a suitable postprocess method has been proposed. Both the first-order and higher order formulations are derived in terms of the first-order shear angle. By assuming that the transverse shear strain energy is the same with both theories, the first-order solution is reinterpreted in terms of the higher order degrees of freedom so as to get a transverse shear distribution that is nearly equivalent to a full higher order solution for the transverse stress distribution. Since the present method needs only the solutions of a first-order shear theory, it is very convenient and easy to calculate through-the-thickness stress distributions. To apply the method to more complicated problems with various geometries and boundary conditions, it is necessary to develop a finite element with the present postprocessor, the development of which is now in progress. An isoparametric element based on FOPT will be implemented with the postprocess method.

Acknowledgments

This research was supported by 1994 Inha University Research Fund. The authors gratefully acknowledge this support. The authors would like to thank a reviewer who gave a thorough and careful reading to the original manuscript.

References

[1]Cho, M., and Parmerter, R. R., "An Efficient Higher-Order Plate Theory for Laminated Composites," *Composite Structures*, Vol. 20, 1992, pp. 113–123.

[2]Lo, K. H., Christensen, R. M., and Wu, E. M., "A Higher Order Theory of Plate Deformation, Part 2: Laminated Plates," *Journal of Applied Mechanics*, Vol. 44, 1977, pp. 669–676.

[3]Krishna Murty, A. V., and Vellaichamy, S., "On Higher Order Shear Laminated Plate Theories," *Composite Structures*, Vol. 8, 1987, pp. 247–270.

[4]Toledano, A., and Murakami, H., "A Composite Plate Theory for Arbitrary Laminate Plate Theory," *Journal of Applied Mechanics*, Vol. 54, No. 1, 1987, pp. 181–189.

[5]Seide, P., "An Improved Approximate Theory for the Bending of Laminated Plates," *Mech. Today*, Vol. 5, 1980, pp. 451–465.

[6]Reddy, J. N., and Barbero, E. J., "A Plate Bending Element Based on a Generalized Laminate Plate Theory," *International Journal for Numerical Methods in Engineering*, Vol. 28, No. 10, 1989, pp. 2275–2292.

[7]Levinson, M., "An Accurate Simple Theory of the Statics and Dynamics of Elastic Plates," *Mechanics Research Communications*, Vol. 7, 1980, pp. 343–350.

[8]Murthy, M. V., "An Improved Transverse Shear Deformation Theory for Laminated Anisotropic Plates," NASA TP 1903, Nov. 1981.

[9]Reddy, J. N., "A Simple Higher-Order Theory for Laminated Composite Plates," *Journal of Applied Mechanics*, Vol. 51, No. 4, 1984, pp. 745–752.

[10]Di Sciuva, M., "Bending Vibration and Buckling of Simply Supported Thick Multilayered Orthotropic Plates: An Evaluation of a New Displacement Model," *Journal of Sound and Vibration*, Vol. 105, No. 3, 1986, pp. 425–442.

[11]Bharska, K., and Varadan, T. K., "Refinement of Higher-Order Laminated Plate Theories," *AIAA Journal*, Vol. 27, No. 12, Dec. 1989, pp. 1831–1841.

[12]Noor, A. K., and Burton, W. S., "Assessment of Shear Deformation Theories for Multilayered Composite Plates," *Applied Mechanics Review*, Vol. 42, No. 1, 1989, pp. 1–13.

[13]Whitney, J. M., "Shear Correction Factors for Orthortopic Laminates Under Static Load," *Journal of Applied Mechanics*, Vol. 40, March 1973, pp. 302–304.

[14]Pagano, N. J., "Exact Solutions for Composite Laminates in Cylindrical Bending," *Journal of Composite Materials*, Vol. 3, July 1969, pp. 398–411.